P-ISSN: 2349-8528
E-ISSN: 2321-4902
www.chemijournal.com
IJCS 2025; 13(1): 03-12

Received: 09-10-2024
Accepted: 15-11-2024

MK Parte
Department of P.G. Studies and Research in Chemistry and Pharmacy, Rani Durgavati Vishwavidyalaya, Jabalpur, Madhya Pradesh, India

PK Vishwakarma
Department of P.G. Studies and Research in Chemistry and Pharmacy, Rani Durgavati Vishwavidyalaya, Jabalpur, Madhya Pradesh, India

RC Maurya
Department of P.G. Studies and Research in Chemistry and Pharmacy, Rani Durgavati Vishwavidyalaya, Jabalpur, Madhya Pradesh, India

Corresponding Author:
PK Vishwakarma
Department of P.G. Studies and Research in Chemistry and Pharmacy, Rani Durgavati Vishwavidyalaya, Jabalpur, Madhya Pradesh, India

Acyl pyrazole and hydrazone derived schiff base and their moo_2 (VI) complex: synthesis, characterization, molecular structural investigations, and insilico biological evaluations

MK Parte, PK Vishwakarma and RC Maurya

Abstract
This research presents the synthesis of the ligand (1Z, N'E)-N'-(cyclohexyl (5-hydroxy-3-methyl-1-phenyl-4, 5-dihydro-1H-pyrazol-4-yl) methylene)-2-hydroxybenzohydrazonic acid (H_3L) and its complex, cis-[MoO_2 (HL) (Me OH)] [C1]. The physicochemical, spectral, and electrochemical evaluations suggested the molecular formula of the complex. DFT-based geometrical computations clarified the molecular structure of the compound. It was found that the ligand coordinates through the azomethine nitrogen and two enolic oxygen of the Schiff base moiety, maintaining a 1:1 ratio with the metal. Furthermore, the title compounds exhibited bioactivity scores and drug-likeness as determined by Molinspiration software, along with ADME properties that suggest potential pharmacological activity.

Keywords: Synthesis, ligand, molybdenum complex, DFT, bioactivity, ADME, pharmacological.

Introduction
Metals play a crucial role as cellular constituents that have been naturally selected to participate in various vital biochemical processes within living organisms. These metals possess distinctive properties, such as redox activity, diverse coordination modes, and reactivity with organic substrates. The application of metals and their salts for therapeutic purposes has been a consistent aspect of human history, spanning from the era of iatrochemistry to contemporary medicine [1]. The active sites of these enzymes generally feature cis-dioxomolybdenum(VI) cation, which is associated with one oxo group and one or two molybdopterin ligands [2]. To replicate the enzymatic activity, researchers have synthesized new model compounds that incorporate a high valent $[MoO_2]^{2+}$ core [3]. Molybdenum dioxo Schiff base complexes are recognized as outstanding models for the active sites of transferase enzymes, particularly nitrate reductase, which contains a cis-MoO2 moiety within its active site [4]. In addition, the biological properties of these complexes have also been explored. For instance, molybdenum complexes formed from ONO donor arylhydrazones were examined for their *in vitro* cytotoxic and antibacterial effects. Similarly, molybdenum complexes utilizing an ONS donor thiosemicarbazone have been shown to serve as models for the active sites of oxo-transfer molybdoenzymes [5, 6].
ADMET, which stands for absorption, distribution, metabolism, excretion, and toxicity, is a fundamental concept in pharmacology. It encompasses the processes by which drugs are handled by the body, impacting their concentration, kinetics, and therapeutic efficacy. Absorption refers to the process by which a drug enters the bloodstream, a process that is affected by variables such as solubility and the passage through the gastrointestinal tract. Distribution pertains to the dispersion of drugs throughout the body, influenced by factors including blood circulation and the molecular characteristics of the substances [7].
The current research outlines the synthesis of a Schiff base formed from 4-(cyclohexanecarbonyl)-3-methyl-1-phenyl-1H-pyrazol-5(4H)-one and salicylic acid hydrazide, as well as its corresponding dioxidomolybdenum(VI) complex. Characterization techniques employed include FT-IR, 1H-NMR, UV-Visible spectroscopy, magnetic moment measurements, and electrochemical analysis. Furthermore, in silico evaluations of the bioactivity and pharmacological properties of the synthesized compounds were conducted.

Experimental Works

The reagents and solvents utilized in this study were procured commercially and were of analytical reagent (AR) grade quality. Microanalytical and NMR spectral analyses were conducted at the Central Drug Research Institute (CDRI) in Lucknow. FTIR spectroscopic data were collected using a Bruker αT FT-IR spectrophotometer with KBr pellets. Electronic absorption measurements were performed with a Varian Cary 5000 UV/Vis/NIR spectrophotometer. Electrochemical assessments were carried out employing TBAP as a supporting electrolyte with an Epsilon BASi cyclic voltameter. The decomposition temperature was determined using a melting point apparatus capable of reaching temperatures up to 360 °C, located within our department. The synthesis of the pyrazoline derivative followed the methodology established by the Maurya group [8].

Synthesis of Schiff base and its Mo (VI) complex [C1]

The Schiff base ligand was synthesized by combining equimolar amounts of 4-(cyclohexanecarbonyl)-3-methyl-1-phenyl-1H-pyrazol-5(4H)-one (570 mg, 2 mmol) with salicylic acid hydrazide (304 mg, 2 mmol). This mixture was subjected to constant stirring and refluxed in methanol for a duration of 4 to 5 hours. The resulting solutions yielded brown precipitates, designated as H_3L. The desired compound was subsequently filtered, washed multiple times with methanol, and dried in a desiccator over anhydrous CaCl2. The complex [C1] was formed by reacting equimolar quantities of [MoO_2 (acac) $_2$] (326 mg, 1 mmol) with the aforementioned Schiff base H_3L, (419 mg, 1 mmol) in a hot methanolic solution. This mixture was refluxed for 4 hours at 60°C, after which it was concentrated to half its original volume and allowed to stand at room temperature for 12 hours. The resulting crystalline solids were filtered, washed with cold methanol, and dried under a vacuum. The compounds were formulated as for H_3LYield; 0.620 g 70%, Colour; Yellow, decomposition temperature; 180 ºC, Anal. Calc. for $C_{24}H_{26}O_4N_3$ (MW: 418.12); C, 64.18; H, 4.29; N, 12.98 Found: C, 68.88; H, 6.26 N, 13.39%. Solubility; Methanol, Ethanol, Acetonitrile, DMF, and DMSO and [C1] Yield; 0.452; 60.4%, Colour; yellow, decomposition temperature; 280 ºC, Anal. Calc. for $C_{25}H_{28}O_6N_4SMo$ (MW: 576); C, 48.06; H, 3.54; N, 9.64 Found: C, 49.52; H, 3.90 N, 9.72%. Solubility; Methanol, Ethanol, Acetonitrile, DMF, and DMSO.

Result and Discussion

The discussion involved the synthesis, formulation, and insilico applied aspects of the Schiff base ligand H_3L and their *cis*-MoO_2 (VI) complex, [MoO_2 (HL)(CH_3OH)] [C1]. The synthetic routes are presented in Scheme 1. Various analytical methods have confirmed the proposed conformation and composition. The Schiff base ligands and their complexes' decomposition temperatures were also tested; the ligand showing a value around 180 ˚C after the completion increase of around 250 ˚C gives clear information about metal-ligand binding.

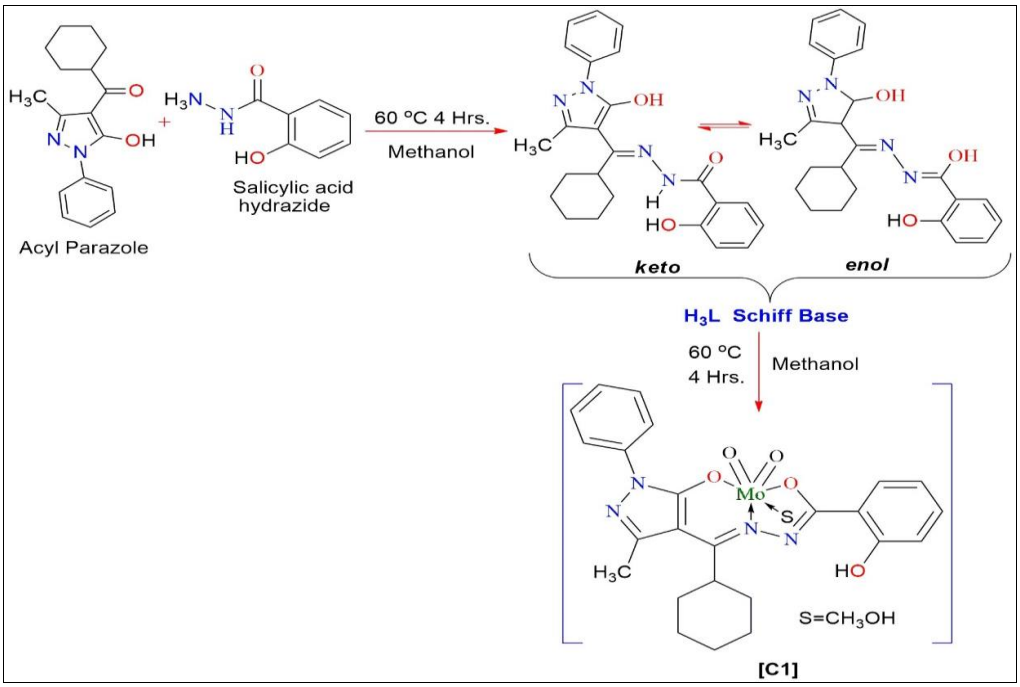

Scheme 1: Synthetic route of Schiff base ligand H_3L & [MoO_2 (HL) (CH_3OH)] [C1].

FT-IR Spectral Analysis

Figure 1, represents the vibrational spectrum of the ligand. In ligand, the three characteristic stretching vibration frequencies are observed as [3432, ν(OH)]; [3280, ν(NH)] and [1580, ν(C=N)] $cm^{-1.}$ After the complexation, the spectral band of [ν(C=N),1588 cm^{-1}] is shifted in lower frequency at ~1570 cm^{-1} in metal complexes suggesting coordination through the azomethine group [9]. The band at 3432 cm^{-1} *ν* (OH) does not appear in the complex, confirming the metal-oxygen coordination. While one more -OH group of the salicylic acid moiety is present in the compounds the bands show at 3442 $cm^{-1.}$ Additionally, the dioxomolybdenum(VI) complexes express a band at 905 and 915 cm^{-1} symmetric and asymmetric mode of (O=Mo=O) representing the occurrence of a *cis*-[MoO_2] group [10,11].

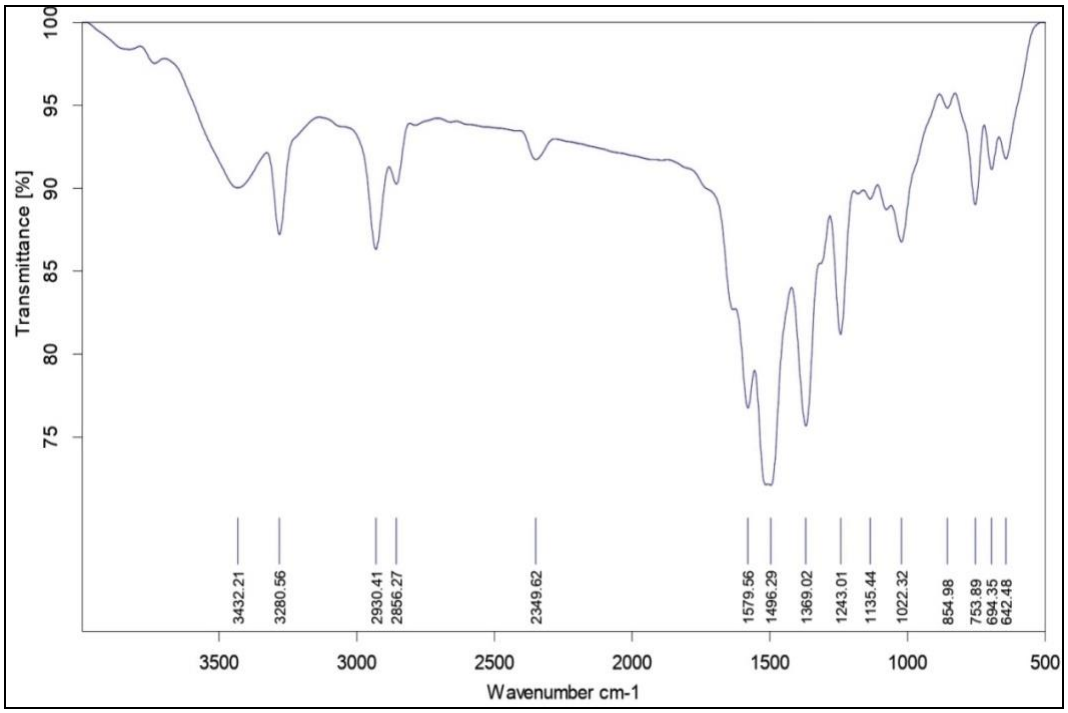

Fig 1: FT-IR spectrum of H_3L.

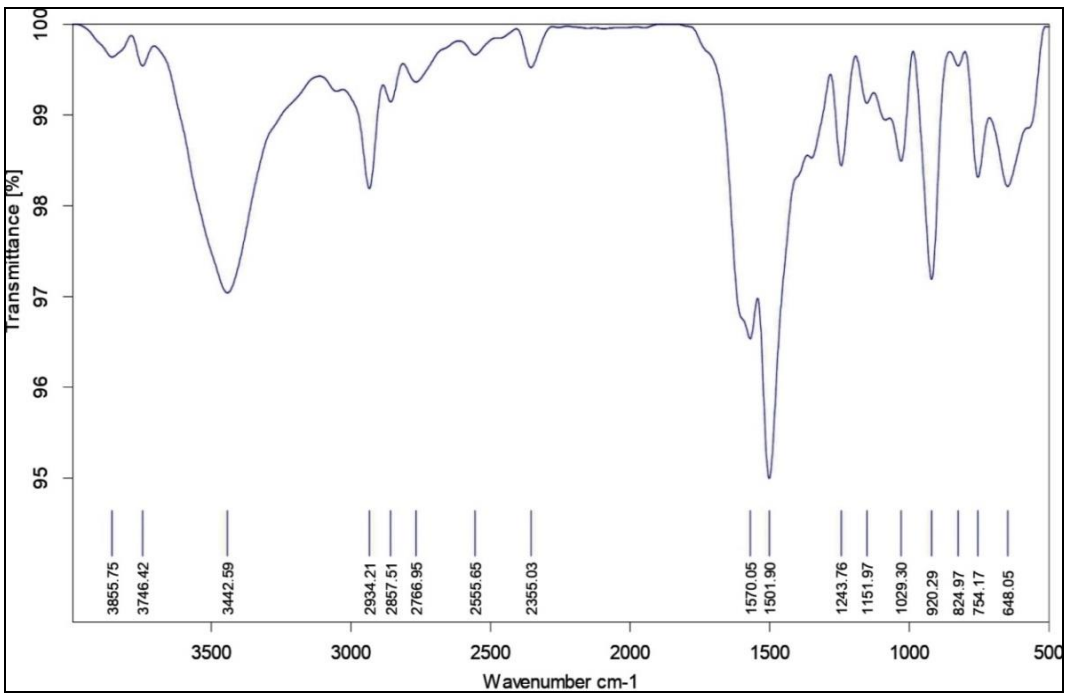

Fig 2: FT-IR spectrum of complex [C1].

Electronic Spectroscopy

The electronic spectral analysis of the complex compound [C1] was conducted in a DMSO solution, with the results illustrated in Figure 3. The compound exhibits two prominent absorption bands in the ultraviolet region, occurring at wavelengths of 268 nm and 328 nm, which can be attributed to π-π* and n-π* transitions, respectively [12, 13]. Additionally, the complex displays a medium-intensity band in the range of 422 nm, which is indicative of a ligand-to-metal charge transfer process [14]. This charge transfer is characterized by the movement of electrons from the filled p-orbitals of the coordinated oxygen atoms to the vacant d-orbitals of the metal, representing a pπ-dπ bonding interaction [15]. Notably, for Mo (VI) complexes, which have a $4d^0$ electronic configuration, the presence of a d-d band is not expected. The magnetic properties of both Mo (VI) complexes are classified as diamagnetic, as evidenced by a magnetic moment measured at zero.

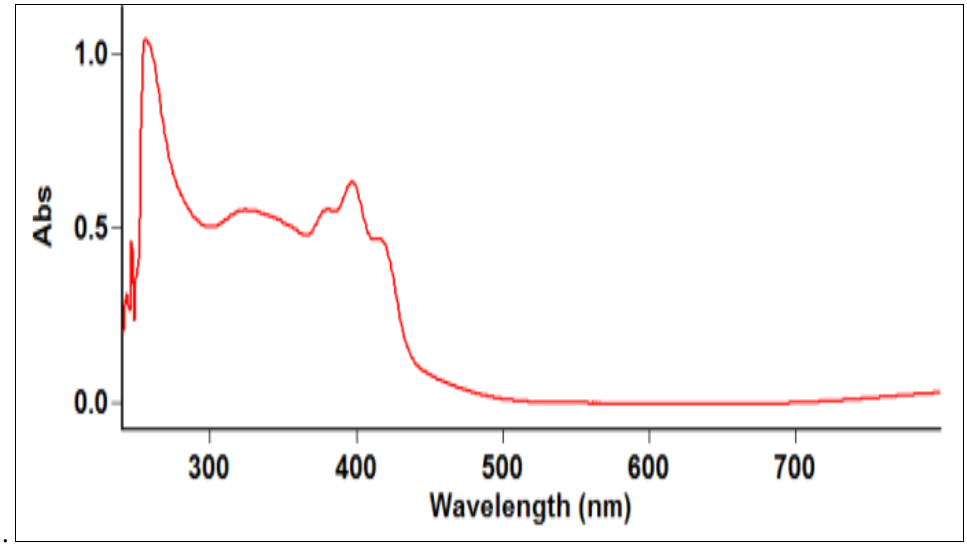

Fig. 3: Electronic Spectrum of *cis*-[MoO_2 (HL)(MeOH)] [C1].

NMR Analysis

Subsequently, the elemental analysis, vibrational frequencies, and the NMR spectral studies supported validating the prepared Schiff base. The ^{1}H-NMR spectrum of the corresponding Schiff base H_3L and their metal complex [C1] were recorded in DMSO- d6 (ppm) and are represented in Figures 4 and 5. The Schiff bases exhibited signals at δ 13.1 (s, 1H, -OH) enolic, and δ 11.3 (s, 1H, -OH) phenolic. A singlet appeared at δ 6.9 ppm due to the (s, 1H, -NH) of the NHCO proton. The aliphatic and aromatic proton signals were detected at δ 2.23 (s, 3H, H_3C-C) and δ7.2 to 7.8 ppm. The multiple singles appeared at δ 1.1-1.9 ppm due to the (s, 5H, C_6H_5) C-H of cyclohexane protons.

In the spectrum of complex [C1] synthesized from H_3L the OH_{enolic} signal at 13.1 ppm disappeared due to involvement in bonding to Mo (VI) centre, and NH signals at 6.9 ppm were also non-existent due to enolization and deprotonation within subsequent coordination into the metal centre the absence of this signal in the complexes also supports the conclusion taken from the IR spectral studies i.e. enolization of the keto group followed by its coordination. The OH_{enolic} signal at 11.3 ppm did not disappear but shifted to the higher side at 11.6 ppm, due to this oxygen atom not bonding to Mo (VI) centre. Moreover, the signal at δ 4.1 and 3.4 ppm was attributed to the OH and CH_3, respectively of coordinated methanol.

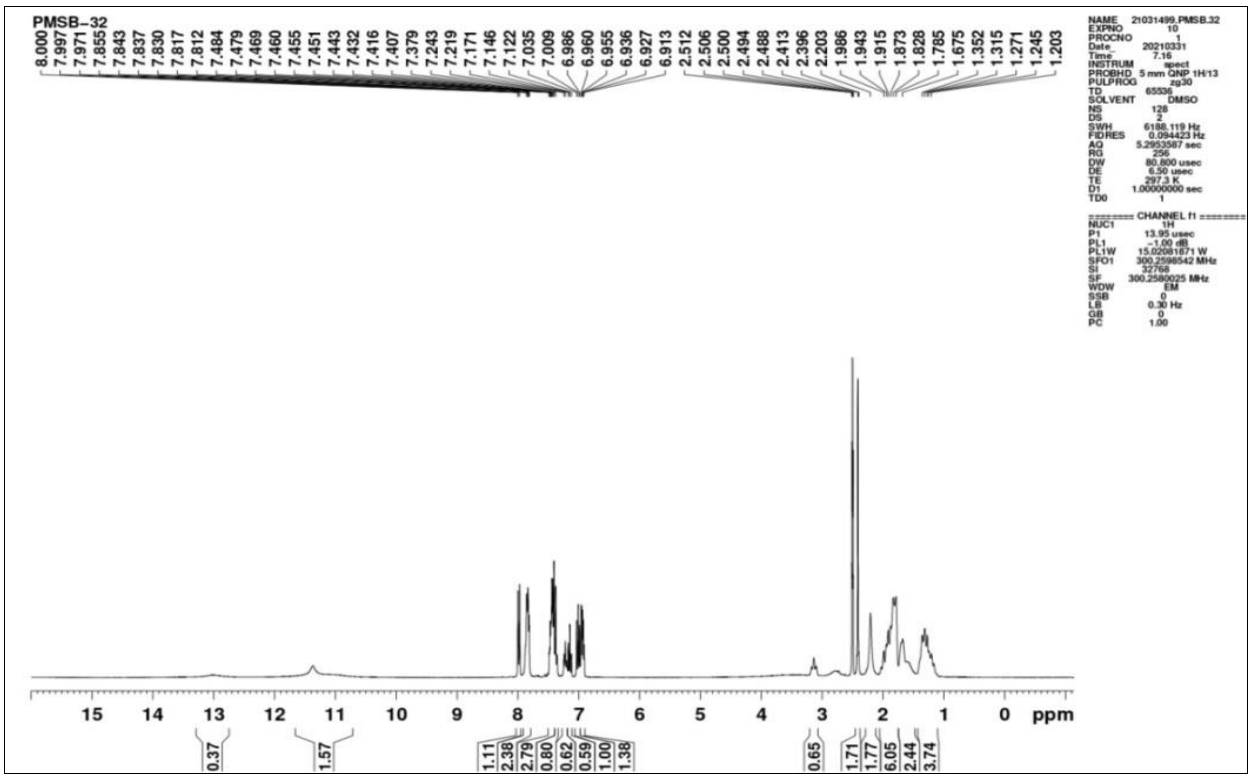

Fig. 4. ^{1}H-NMR spectrum of H_3L.

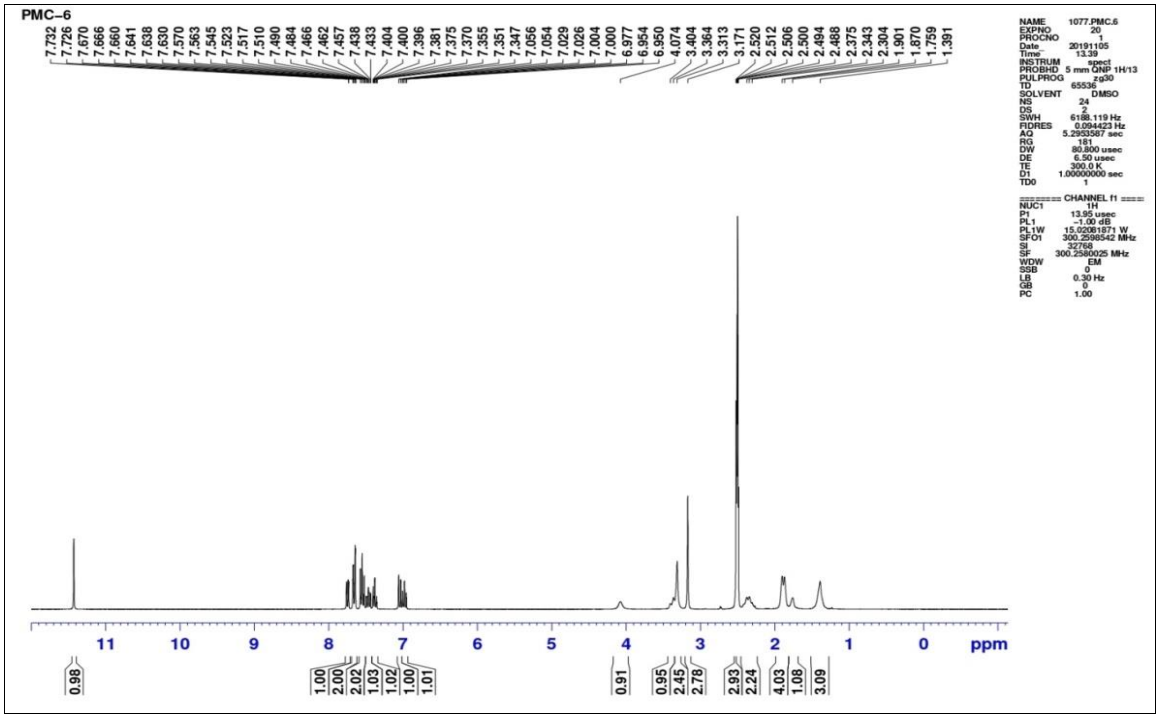

Fig. 5: ^{1}H-NMR spectrum of *cis*-[MoO_2 (HL)(MeOH)] [C1].

^{3}C-NMR spectra of H_3L and their mononuclear Mo (VI) complex, [C1] are presented in Figures 6 and 7, respectively. The signals of the aromatic carbons Ar-C are observed in the range of δ =116.461-138.88 ppm and aliphatic (CH_3-C) carbon is found at δ=17.69 ppm. Apart from the aliphatic and aromatic carbons, the compounds have six cyclohexane carbon atoms in the Schiff base moiety the signals are observed at δ =25.29-30.32 ppm. The signal at δ=157.4 ppm (C-OH) phenolic and δ =155.6 ppm (N=C-CH_3). The three carbon atoms signals are observed at δ =165.19 ppm (N-C=O) amide, δ =146.47 ppm (-N=C-R) hydrazide, and δ 97.1 ppm (C-OH)$_{pyrazoline}$. While in complex the significant chemical shift [Δδ =δ (complex)-δ (ligand)] of the three carbons existing in the vicinity [i.e. C1, C2, and C3 see in the scheme] of the conforming atoms of the ligand confirmed the coordination of $O_{pyrazoline}$, $N_{azomethine,}$ and O_{amide} to the Mo (VI) center. One additional signal has also exhibited at δ=48.55 ppm it assigns the carbon atom of coordinated methanol, confirming that the six-coordination site is occupied by methanol. This is further supported by the appearance of a peak at δ=4.01 ppm of methanolic OH, ^{1}H-NMR spectrum. The whole spectral data and its discussion confirm the coordination of ligands as diprotic ONO donor environments only [16]. The long peaks at δ 40.0 ppm in all the spectra are observed in DMSO as solvent.

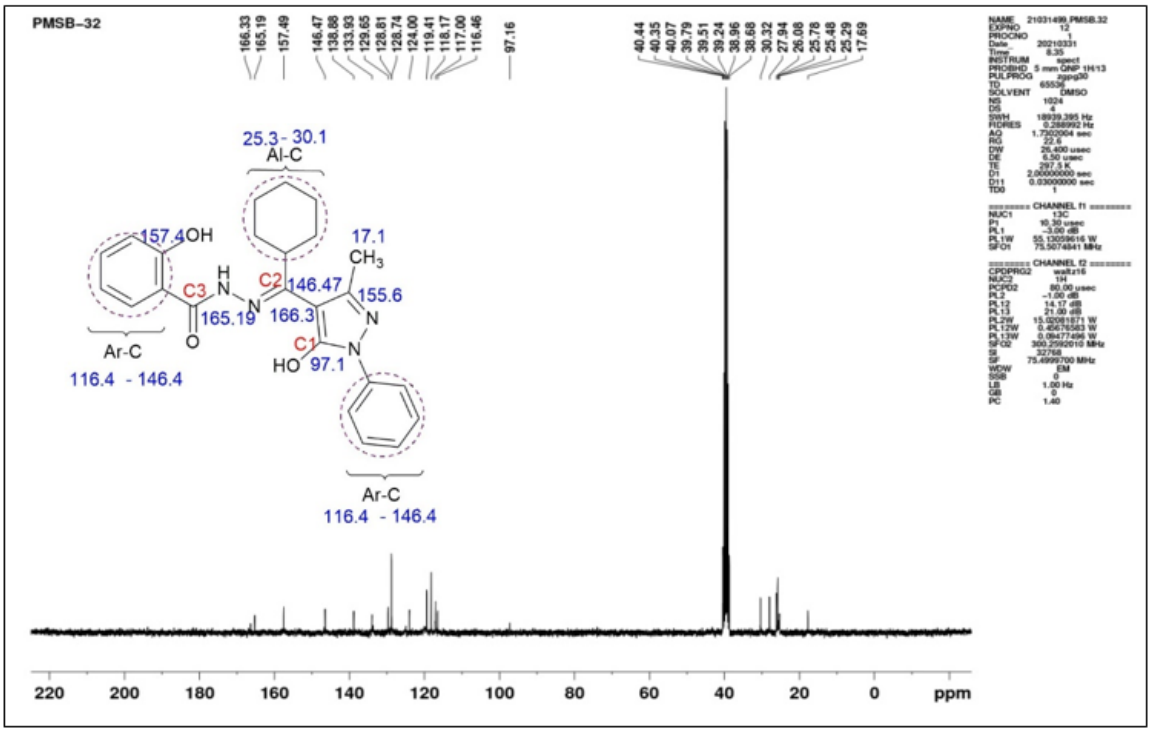

Fig. 6: ^{13}C-NMR spectrum of H_3L.

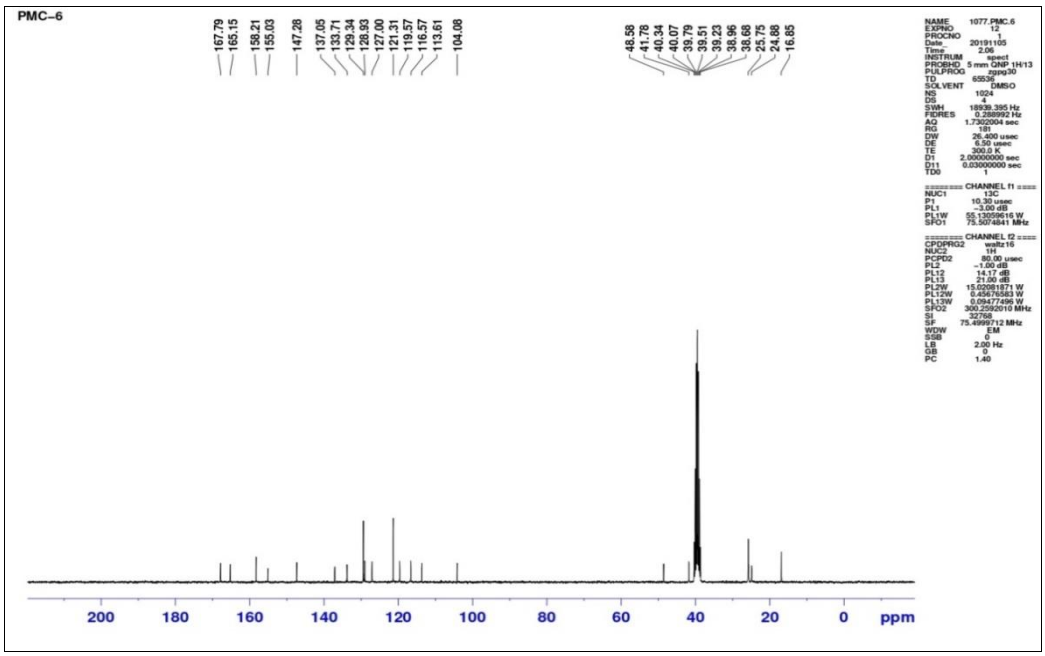

Fig. 7: ^{13}C-NMR spectrum of *cis*-[MoO_2 (HL) (MeOH)] [C1].

Electrochemical Analysis

The electrochemistry of the complex compound [C1] was recorded in DMSO solution using a cyclic voltammogram with the three electrodes with 0.1 M tetra butyl ammonium perchlorate (TBAP) as electrolyte at variable applied scan range in IUPAC mode. The results are illustrated in Table 1. The following two Figure 8 depict the voltammogram [C1] are displayed at different variable scan range in single step an irreversible reduction peak at 100 scan rate mV/s as [E_{pc}(0.192)V; I_{pc}(0.364)µA] that can be determined as $[MoO_2]^{2+}\rightarrow$[MoO_2] and mono step an irreversible oxidation wave as and [E_{pa}(-1.456)V; I_{pa}(-0.664)µA] that can be used to establish as $[MoO_2]\rightarrow [MoO_2]^{2+}$. The formal reduction potential Er is also detected as -0.824 V. The calculated Ipa/Ipc ratios are 1.796 for both complexes in respective order, indicating that these complexes have a reversible redox property [17].

Tab. 1: Electrochemical data of the studied complex [C1].

Comp.	Scan rate mV/s	E_{pc} (V)	I_{pc} (A)	E_{pa} (V)	I_{pa} (μA)	E_r (V)	ΔE (V)	I_{pa}/I_{pc}
[C1]	100	0.192	0.364	-1.456	-0.654	-0.824	1.648	1.796
	200	0.256	0.412	-1.522	-0.722	-0.889	1.778	1.760
	300	0.378	0.506	-1.588	-0.795	-0.983	1.966	1.571

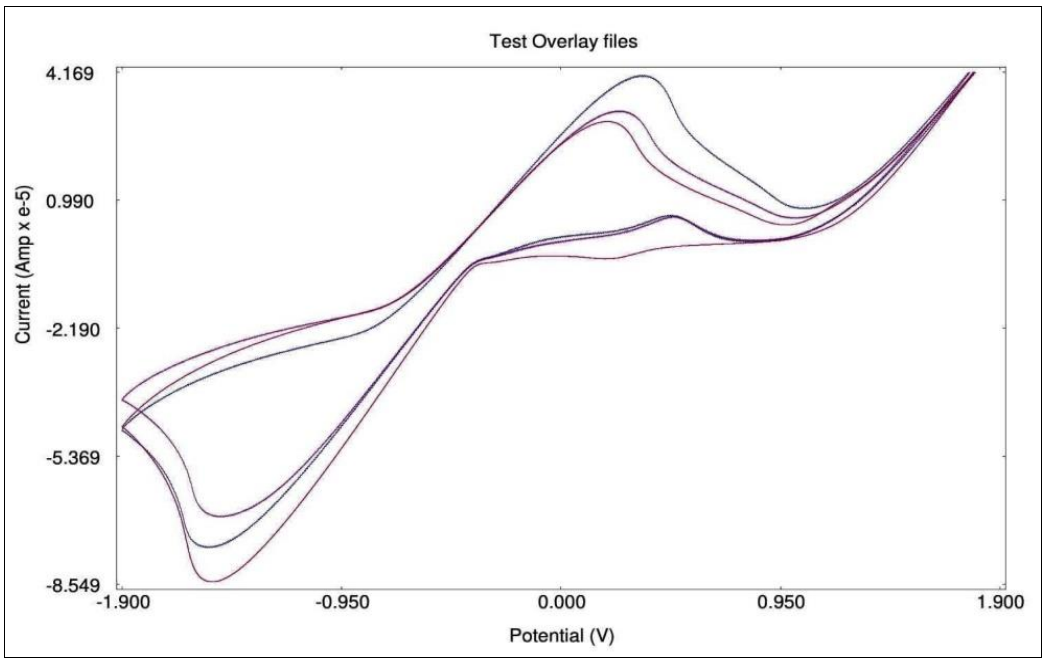

Fig 8: Cyclic voltammogram of synthesized complex [C1].

Molecular Structural Analysis

The molecular geometry of the cis-MoO_2 (VI) complex, designated as [C1], was determined using DFT/LANL2DZ methods via the Gaussian 09 software. The structural representations are illustrated in Figure 9. The complex [C1] features a monomeric Mo (VI) entity characterized by a $[MoO_2]^{2+}$ fragment. The acyl pyrazolone-hydrazone ligand, H_3L, acts as a tridentate dibasic ONO donor ligand. Within the complex, the molybdenum centre exhibits a distorted octahedral configuration, coordinating with three donor atoms from the ligand: the enolic oxygen O (26), the azomethine nitrogen N (10), and another enolic oxygen O (8). Additionally, the molybdenum is bonded to two oxido oxygen atoms, O (25) and O (49). The sixth coordination site is occupied by the oxygen atom O (24) from a coordinated methanol molecule, fulfilling the requirement for molybdenum hexa-coordination. The oxido oxygen atoms O (25) and O (49) are positioned cis to one another, with Mo=O bond lengths measuring 1.742 Å and 1.728 Å, and a bond angle of O=Mo=O at 106.564°, confirming the presence of the *cis*-MoO_2 moiety in the complex. The thirteen selected *cis* bond angles for the complex range from 72.121º to 103.461º, while the three *trans* angles from 146.264º to 170.412º, indicate an irregular geometric configuration. Notwithstanding this, the bond lengths associated with the remaining molybdenum-ligand connections conform well to the bond length range identified in previously reported cis-dioxidomolybdenum complexes [18, 19]. Minor discrepancies in their geometrical outcomes may be attributed to computational effects and experimental conditions.

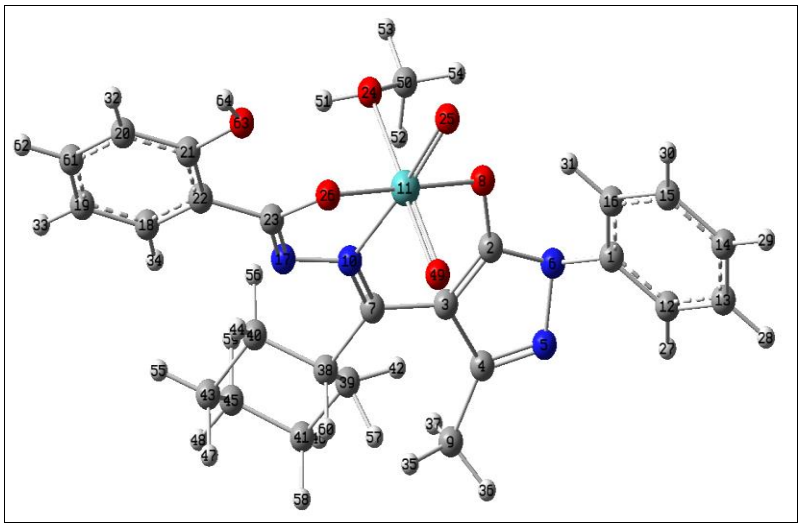

Fig. 9: The optimized molecular structure of the complex [C1].

Insilco Biological Prediction

The pharmacological properties of drugs are characterized by their significant interactions with a variety of biological targets, such as enzymes, ion channels, and receptors within living organisms. The bioavailability of the compounds in question was estimated through a computational analysis conducted on the web platform www.molinspiration.com, with the findings presented in Table 2. The evaluation of bioactivity scores is based on five specific parameters. (a) G-protein coupled receptor ligand (GPCRL) (b) Ion channel modulation (ICM) (c) Nuclear Receptor Ligand (NRL), (d) Protease Inhibition (PI) and Enzyme Inhibition (EI).

Recent studies have established that substances with bioactivity scores of 0.0 or higher are categorized as highly bioactive, while those with scores between 5.0 and 0 are considered to have moderate bioactivity. In contrast, compounds scoring 0.5 or lower are classified as inactive [20]. The compounds in question exhibit bioactivity scores ranging from -0.53 to -0.03, indicating a prediction of moderate activity [21]. It is expected that these compounds will retain their bioactive characteristics, contingent upon certain modifications to their molecular structures [22]. Additionally, Lipinski's rule [23] of five (RO5) provides a foundational guideline for drug design and development, detailing the molecular attributes that correlate with key pharmacokinetic parameters, including absorption, distribution, metabolism, and excretion (ADME). This rule is instrumental in forecasting the success of orally administered drugs as they navigate through the body to their sites of action. (a) MlogP (partition coefficient), (b) Molecular weight, (c) Number of hydrogen bond acceptors (nON), (d)Hydrogen bond donors (nOHNH), and (e) Topological Polar Surface Area (TPSA). The rule of five (RO5) serves as a guideline for predicting the oral bioavailability of the compounds. For a medicine to be considered orally active, it should adhere to specific criteria: a MlogP value of 5 or less, a maximum of 10 hydrogen bond acceptors, no more than 5 hydrogen bond donors, and a molecular weight of approximately 500. Typically, an orally active drug should not violate these rules. In this study, the% absorption, TPSA, milLogP, and other relevant parameters of the title compound are calculated and presented in Table 3. The calculation of percentage absorption (% abs.) was performed using the formula% Abs = 109 - [0.345 × TPSA]. Here, the topological polar surface area (TPSA) is defined as the cumulative surface area of polar atoms within a molecule. The criteria are primarily influenced by various factors, including molecular weight, which should be less than 500 Da, and topological polar surface area, which ranges from 60 to 140 $Å^2$ [24]. Additionally, the analysis considered the logarithm of the compound's partition coefficient between n-octanol and water, the number of hydrogen bond donors (nOHNH), the number of hydrogen bond acceptors (nON), and the total count of rotatable bonds (nrotb).

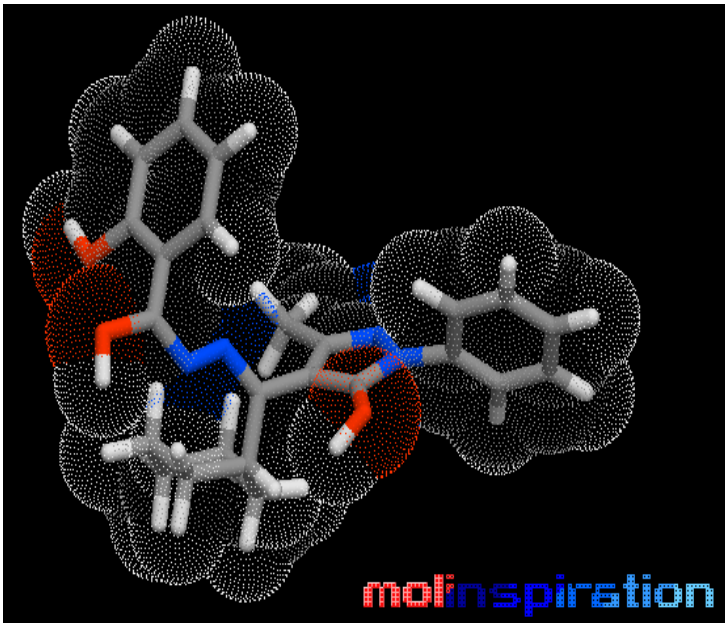

H_2L

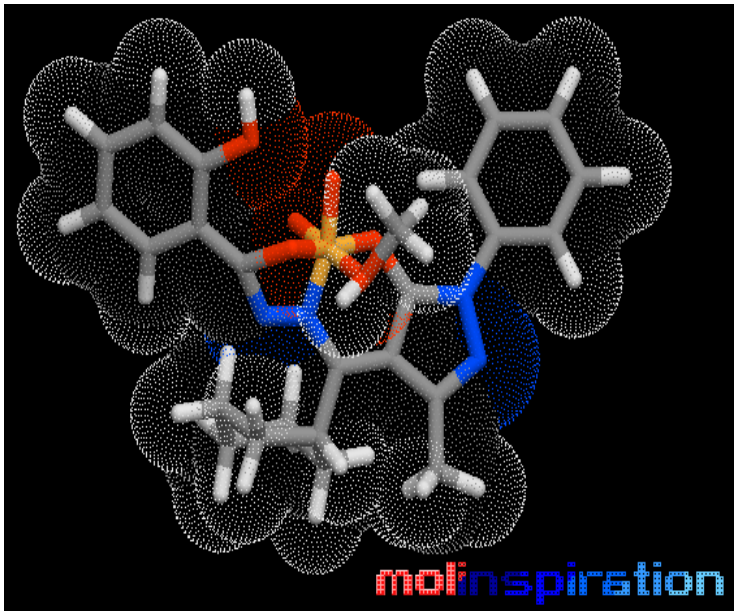

[C1]

Fig 9: 3D-Molecular structures of title ligand and their metal complex obtained through Molinspiration galaxy 3D structure generator v2021.01 beta a web tool.

Table 2: Bioactivity score of the synthesized ligand and their complex [C1].

Comp.	Parameters of Bioactivity Score					
	GPCR ligand	Ion channel modulator	Kinase inhibitor	Nuclear receptor ligand	Protease inhibitor	Enzyme inhibitor
H_3L	-0.25	-0.35	-0.53	-0.48	-0.31	-0.23
[C1]	-0.03	-0.12	-0.16	-0.21	-0.12	-0.06

Table 3: Bioactivity score of the synthesized ligand and their complex C1.

Comp.	Lipinski's Parameters							
	% Abs.	TPSA (Å)^2	MlogP	nOHNH	nON	nrtb	Mwt.	Lipinski's violations
H_3L	73.38	103.24	4.71	3	7	5	418.50	0
[C1]	67.48	120.36	-2.82	2	10	4	576.46	1

After the Insilco biological activity of the title compound one more computer-aided technique was used to predict ADME properties by ADMETSAR methodology [25] web server (http://lmmd.ecust.edu.cn/admetsar2). The method is performed to investigate whether the investigated compounds produce any toxicity after administration in the body or show any pharmacokinetic profile. This methodology is based on the molecular structure of the

compounds that were characterized for the prediction of their pharmacokinetics, absorption, distribution, metabolism, and excretion (ADME) and their pharmacodynamics and toxicity, to avoid potential interactions of drugs with anti-targets causing many side effects. Here various ADME models namely: (a) Blood-brain barrier (BBB) penetration (b) Aqueous solubility (LogS) (c) Caco-2 cell permeability, (d) Human Intestinal Absorption (HIA), (e) Carcinogenetic and (f) LD50 dosage
The predicted ADMET data of the title compounds are charted in Table 4. The compounds show high absorption, and distribution properties indicated by the higher value of HIA, BBB, and Caco2 permeability values, and it suggests the more auspicious pharmacokinetic properties. The carcinogenic profile of compounds also displayed a non-carcinogenic nature. One of the more applied features collected from ADMETSAR is the computed median lethal dose (LD50) dosage in the rat model (acute rat toxicity) which helps in deciding the lethalness of compounds. The lower the LD50 value, the more lethal the compounds are in comparison to those with higher LD50 values. The LD50 values of the compounds examined are typically higher than that of the drug streptomycin, which has an LD50 of 1.841 mol/kg.

Table 4: ADMET activity score of the Schiff base ligand and metal complex.

Comp.	BBB	HIA	Caco2	ROCT	Carcinogenicity	LogS	LD50 mol/kg
H_3L	0.8118	0.9952	0.5385	Non-inhibitor	Non-carcinogens	-0.8072	2.2806
[C1]	0.5927	0.6990	0.5831	Non-inhibitor	Non-carcinogens	-3.3994	2.6043

Conclusions
This research work concludes with a discussion on the synthesis, characterization, and computational exploration of pyrazoline and salicylic acid hydrazide, including the Schiff base and its associated MoO_2 complex. The molecular formulae of the mononuclear MoO_2 (VI) complex, referred to as [MoO_2 (HL) (Me OH)] [C1], was established through geometrical evaluations conducted via the DFT method. The findings from both spectroscopic and computational analyses reveal that the complex possesses a distorted octahedral geometry with a 1:1 stoichiometric ratio of metal to ligand. Additionally, the applications of the compounds are informed by in silico bioactivity and ADME results, indicating promising pharmacokinetic profiles and biological activities. The bioactivity scores for the compounds range from -0.48 to -0.03, while the TPSA values for H_3L and [C1] are 103.24 and 120.36 Å², respectively. The LD50 values for the compounds are 2.2806 and 2.6043, which are higher than that of the commonly utilized drug streptomycin (LD50=1.841 mol/kg).

Acknowledgment
The authors wish to convey their sincere appreciation to Professor P.K. Khare, the Head of the Department, for providing the crucial analytical resources necessary for this work. Furthermore, they express their gratitude to Prof. Rajesh Kumar Verma, Vice Chancellor of Rani Durgavati Vishwavidyalaya Jabalpur, for his encouragement and unwavering support.

Conflicts of Interest
The authors indicated that there were no potential conflicts of interest to declare.

Funding
No funding for this work.

References
1. Frezza M, Hindo S, Chen D, Davenport A, Schmitt S, Tomco D, Dou QP. Novel metals and metal complexes as platforms for cancer therapy. Curr Pharm Des. 2010;16(16):1813-1825.
2. Hille R. The reaction mechanism of oxomolybdenum enzymes. Biochim Biophys Acta. 1994;1184:143-169.
3. Dupe A, Judmaier ME, Belaj F, Zangger K, Mosch-Zanetti NC. Activation of molecular oxygen by a molybdenum complex for catalytic oxidation. Dalton Trans. 2015;44:20514-20522.
4. Hossain MK, Haukka M, Sillanpaa R, Hrovat DA, Richmond MG, Nordlander E, *et al.* Syntheses and catalytic oxotransfer activities of oxo molybdenum(VI) complexes of a new aminoalcohol phenolate ligand. Dalton Trans. 2017;46:7051-7060.
5. Asha TM, Kurup MRP. Syntheses and catalytic oxotransfer activities of oxo molybdenum(VI) complexes of a new aminoalcohol phenolate ligand. Polyhedron. 2019;169:151.
6. Asha TM, Kurup MRP. An insight into the potent antioxidant activity of a dithiocarbohydrazone appended cis-dioxidomolybdenum(VI) complexes. Appl Organomet Chem. 2020;e5762. doi:10.1002/aoc.5762.
7. Kaavin K, Naresh D, Yogeshkumar MR, Krishna Prakash M, Janarthanan S, Murali Krishnan M, *et al.* In-silico DFT studies and molecular docking evaluation of benzimidazo methoxy quinoline-2-one ligand and its Co, Ni, Cu and Zn complexes as potential inhibitors of Bcl-2, Caspase-3, EGFR, mTOR, and PI3K, cancer-causing proteins. Chem Phys Impact. 2024;8:100418.
8. Mir JM, Maurya RC, Vishwakarma PK, Rajak DK, Jain N, Jaget PS, *et al.* Synthesis and conjoint experimental - DFT characterization of some pyrazolone functionalized dioxovanadium(V) Schiff base complexes. J Theor Comput Sci. 2016;3. doi:10.4172/2376-130X.1000147.
9. Mishra AP, Mishra RK, Shrivastava SP. Structural and antimicrobial studies of coordination compounds of VO (II), Co(II), Ni(II) and Cu(II) with some Schiff bases involving 2-amino-4-chlorophenol. J Serb Chem Soc. 2009;74(5):523-535.
10. Ceylan BI, Kurt YD, Ulkuseyen B. Synthesis and characterization of new dioxomolybdenum(VI) complexes derived from benzophenone thiosemicarbazone (H2L). Crystal structure of [MoO2L (PrOH)]. J Coord Chem. 2009;62(5):757-766.
11. Maurya MR, Tomar R, Gupta P, Avecilla F. Trinuclear cis-dioxidomolybdenum(VI) complexes of compartmental C3 symmetric ligands: Synthesis, characterization, DFT study and catalytic application for hydropyridines (Hps) via the Hantzsch reaction. Polyhedron. 2020;186:114617.

12. Dawar N, Devi J, Kumar B, Dubey A. Synthesis, characterization, pharmacological screening, molecular docking, DFT, MESP, ADMET studies of transition metal(II) chelates of bidentate Schiff base ligand. Inorg Chem Commun. 2023;151:110567.
13. Guleryuz C, Sumrra SH, Hassan AU, Nkungli NK, Muhsan MS, Alshehri SM. Excited state dependent fast switching NLO behavior investigation of sp2 hybridized donor crystal as D-π-A push-pull switches. Results Chem. 2024;7:101382.
14. Syamal A, Maurya MR. New dioxomolybdenum(VI) complexes with tridentate dibasic ONO donor Schiff bases. Indian J Chem. 1986;25A:1152-1155.
15. Maurya MR, Rana L, Avecilla F. Phloroglucinol and resorcinol-based mononuclear dioxidomolybdenum(VI) complexes: Synthesis, structural characterization, and catalytic epoxidation. Polyhedron. 2017;126:60-71.
16. Maurya MR, Dhaka S, Avecilla F. Oxidation of secondary alcohols by conventional and microwave-assisted methods using molybdenum complexes of ONO donor ligands. New J Chem. 2015;39:2130-2139.
17. Ngan NK, Lo KM, Wong CSR. Dinuclear and polynuclear dioxomolybdenum(VI) Schiff base complexes: Synthesis, structural elucidation, spectroscopic characterization, electrochemistry, and catalytic property. Polyhedron. 2012;33:235-251.
18. Asha TM, Kurup MRP. Synthesis, spectroscopy, electrochemistry, crystal structures and *in vitro* cytotoxicity of mononuclear molybdenum (VI) complexes incorporating tridentate ONO donor aroylhydrazone with auxiliary coordination site. Inorgan Chim Acta. 2018;483:44-52.
19. Pasayat S, Dash PS, Saswati, Majhi PK, Patil YP, Nethaji M, *et al.* Mixed-ligand aroylhydrazone complexes of molybdenum: Synthesis, structure and biological activity. Polyhedron. 2012;38:198-204.
20. Venturini A, Gonzalez J. A CASPT2 and CASSCF approach to the cycloaddition of ketene and imine: A new mechanistic scheme of the Staudinger reaction. J Org Chem. 2002;67:9089-9092.
21. Dhanaraj CJ, Johnson J. Studies on some metal complexes of quinoxaline-based unsymmetric ligand: Synthesis, spectral characterization, *in vitro* biological and molecular modeling studies. J Photochem Photobiol B Biol. 2016;161:108-121.
22. Vishwakarma PK, Maurya RC. Synthesis, characterization and DFT studies of Schiff base (E)-4-(((5-hydroxy-3-methyl-1-phenyl-1H-pyrazol-4-yl) methylene) amino)-benzenesulfonamide and its MoO2 (II) complex. J Res Chem. 2023;4(1):47-55.
23. Lipinski CA. Lead- and drug-like compounds: The rule-of-five revolution. Drug Discov Today Technol. 2004;1(4):337-341.
24. Veber DF, Johnson SR, Cheng HY, Smith BR, Ward KW, Kopple KD. Molecular properties that influence the oral bioavailability of drug candidates. J Med Chem. 2002;45(12):2615-2623.
25. Cheng F, Li W, Zhou Y, Shen J, Wu Z, Liu G, *et al.* admetSAR: A comprehensive source and free tool for assessment of chemical ADMET properties. J Chem Inf Model. 2012;52:3099-3105.